ROBUST STABILIZATION OF A QUADROTOR UAV IN PRESENCE OF ACTUATOR AND SENSOR FAULTS

Hicham Khebbache [1], Belkacem Sait [2], Naâmane Bounar [3] and Fouad Yacef [4]

[1,2] Automatic Laboratory of Setif (LAS), Electrical Engineering Department, Setif University, ALGERIA

khebbachehicham@yahoo.fr , sait_belkacem19@yahoo.fr

[3,4] Automatic Laboratory of Jijel (LAJ), Automatic Control Department, Jijel University, ALGERIA

bounar18@yahoo.fr , yaceffouad@yahoo.fr

ABSTRACT

This paper deals with the stabilization problem of an underactuated quadrotor UAV system in presence of actuator and sensor faults. The dynamical model of quadrotor while taking into account various physical phenomena, which can influence the dynamics of a flying structure is presented. Subsequently, a new control strategy based on backstepping approach, taking into account the actuator and sensor faults is developed. Lyapunov based stability analysis shows that the proposed control strategy design keeps the stability of the closed loop dynamics of quadrotor UAV even after the presence of these faults. Simulations of the controlled system, illustrate that the proposed control strategy is able to maintain performance levels and to preserve stability under the occurrence of actuator and sensor faults.

KEYWORDS

Actuator faults, Backstepping control, Dynamic model of quadrotor, Fault tolerant control (FTC), Robust control, Sliding mode control, Sensor faults,Unmanned aerial vehicles (UAV).

1. INTRODUCTION

Unmanned aerial vehicles (UAV's) offer challenging benchmark control problems and have been the focus for many researchers in the past few years [2]. They are being used more often for military and civilian purposes such as traffic monitoring, patrolling for forest fires, surveillance, and rescue, in which risks to pilots are often high. Moreover, small quadrotor helicopters possess a great maneuverability and are potentially simpler to manufacture. For these advantages, quadrotor helicopters have received much interest in UAV research.

The quadrotors, has been studied recently by some authors [14], [8], [2], [15], [16], [11], [20], [3], [4], [1], [6], [12], [17], [10], [13], [9], [18], [7], [5]. These systems as many other dynamic systems, present constant or slowly-varying uncertain parameters, but these authors do not take into account the faults affecting the actuators and sensors of our system, wich makes them very limited and induces undesired behavior of quadrotor, or even to instability of the latter after occurence of actuator and sensor faults.

DOI : 10.5121/ijics.2012.2205

In this paper, the stabilization problem of the quadrotor aircraft in presence of actuator and sensor faults is considered. The dynamical model describing the quadrotor aircraft motions and taking into a account for various parameters which affect the dynamics of a flying structure is presented. Subsequently, a new control strategy based on backstepping approach taking into account the actuator and sensor faults is developed. This control strategy includes two compensation techniques, the first one is to use an integral compensation term, and the second technique by using an another compensation term containing "sign" function. Finally all synthesized control laws are highlighted by simulations which gave fairly satisfactory results despite the occurrence of simultaneous actuator and sensor faults.

2. DYNAMICAL MODEL

2.1. Quadrotor dynamic model

The quadrotor have four propellers in cross configuration. The two pairs of propellers {1,3} and {2,4} as described in Figure. 1, turn in opposite directions. By varying the rotor speed, one can change the lift force and create motion. Thus, increasing or decreasing the four propeller's speeds together generates vertical motion. Changing the 2 and 4 propeller's speed conversely produces roll rotation coupled with lateral motion. Pitch rotation and the corresponding lateral motion; result from 1 and 3 propeller's speed conversely modified. Yaw rotation is more subtle, as it results from the difference in the counter-torque between each pair of propellers.

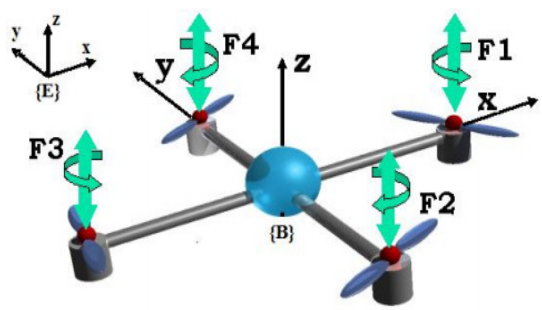

Figure 1. Quadrotor configuration

The quadrotor model (position and orientation dynamic) obtained is given like in [3], [4], [5] by:

$$\begin{cases} \ddot{\phi} = \dfrac{(I_y - I_z)}{I_x}\dot{\theta}\dot{\psi} - \dfrac{J_r}{I_x}\bar{\Omega}_r\dot{\theta} - \dfrac{K_{fax}}{I_x}\dot{\phi}^2 + \dfrac{l}{I_x}u_2 \\ \ddot{\theta} = \dfrac{(I_z - I_x)}{I_y}\dot{\phi}\dot{\psi} + \dfrac{J_r}{I_y}\bar{\Omega}_r\dot{\phi} - \dfrac{K_{fay}}{I_y}\dot{\theta}^2 + \dfrac{l}{I_y}u_3 \\ \ddot{\psi} = \dfrac{(I_x - I_y)}{I_z}\dot{\theta}\dot{\phi} - \dfrac{K_{faz}}{I_z}\dot{\psi}^2 + \dfrac{1}{I_z}u_4 \\ \ddot{x} = -\dfrac{K_{ftx}}{m}\dot{x} + \dfrac{1}{m}u_x u_1 \\ \ddot{y} = -\dfrac{K_{fty}}{m}\dot{y} + \dfrac{1}{m}u_y u_1 \\ \ddot{z} = -\dfrac{K_{ftz}}{m}\dot{z} - g + \dfrac{\cos(\phi)\cos(\theta)}{m}u_1 \end{cases} \tag{1}$$

with

$$\begin{cases} \bar{\Omega}_r = \omega_1 - \omega_2 + \omega_3 - \omega_4 \\ u_x = (\cos\phi\cos\psi\sin\theta + \sin\phi\sin\psi) \\ u_y = (\cos\phi\sin\theta\sin\psi - \sin\phi\cos\psi) \end{cases} \tag{2}$$

u_1, u_2, u_3 and u_4 are the control inputs of the system which are written according to the angular velocities of the four rotors as follows:

$$\begin{bmatrix} u_1 \\ u_2 \\ u_3 \\ u_4 \end{bmatrix} = \begin{bmatrix} b & b & b & b \\ 0 & -lb & 0 & lb \\ -lb & 0 & lb & 0 \\ d & -d & d & -d \end{bmatrix} \begin{bmatrix} \omega_1^2 \\ \omega_2^2 \\ \omega_3^2 \\ \omega_4^2 \end{bmatrix} \tag{3}$$

From (2) it easy to show that :

$$\begin{cases} \phi_d = \arcsin\left(u_x \sin(\psi_d) - u_y \cos(\psi_d)\right) \\ \theta_d = \arcsin\left(\dfrac{\left(u_x \cos(\psi_d) + u_y \sin(\psi_d)\right)}{\cos(\phi_d)}\right) \end{cases} \tag{4}$$

2.2. Rotors dynamic model

The dynamics of a DC motor is given by the following differential equations:

$$J_r \dot{\omega}_i = \tau_i - Q_i , \ i \in \{1,2,3,4\} \tag{5}$$

With $Q_i = d\omega_i^2$ is the reactive torque generated, in free air, by the rotor i due to rotor drag, and τ_i is the input torque.

A control law for the input torque τ_i is developed in [20], it is given by:

$$\tau_i = Q_i + J_r \dot{\omega}_{d,i} - k_i \tilde{\omega}_i \tag{6}$$

where k_i, i∈{1,…,4} are four positive parameters, $\omega_{d,i}$, i∈{1,…,4} are the desired speed of each rotor and $\tilde{\omega}_i = \omega_i - \omega_{d,i}$.

In fact, applying (6) to (5) leads to

$$\dot{\tilde{\omega}}_i = -\frac{k_i}{J_r} \tilde{\omega}_i \tag{7}$$

which shows the exponential convergence of ω_i to $\omega_{d,i}$ and hence the convergence of the airframe torques to the desired values leading to the attitude stabilization of the quadrotor aircraft.

In our application, the DC motors are voltage controlled. Assuming that the motor inductance is small and taking into consideration the gear ratio, one can obtain the voltage to be applied to each motor as follows [20]:

$$v_i = \frac{R_a}{k_m k_g}\tau_i + k_m k_g \omega_i, \; i \in \{1,2,3,4\} \tag{8}$$

where R_a is the motor resistance, k_m is the motor torque constant, and k_g is the gear ratio.

3. CONTROL STRATEGY OF QUADROTOR WITH ACTUATOR FAULTS

The complete model resulting by adding the actuator and sensor faults in the model (1) can be written in the state-space form:

$$\begin{cases} \dot{x}(t) = \eta(x,t) + g(x,t)\big(u(t) + f_a(t)\big) \\ y(t) = h(x,t) + f_s(t) \end{cases} \tag{9}$$

With $x(t) \in \Re^n$ is the state vector of the system, $y(t) \in \Re^p$ is the measured output vector, $u(t) \in \Re^m$ is the input control vector, $f_a(t) \in \Re^{q_a}$ is the resultant vector of actuator faults related to quadrotor motions and $f_s(t) \in \Re^{q_s}$ is the sensor faults vector, such as:

$$x = [x_1, \ldots, x_{12}]^T = \left[\phi, \dot{\phi}, \theta, \dot{\theta}, \psi, \dot{\psi}, x, \dot{x}, y, \dot{y}, z, \dot{z}\right]^T \tag{10}$$

Remark 1: In our contribution, only the velocity sensor faults are considered.

From (1), (10) and considering the actuator and velocity sensor faults, we obtain :

$$\begin{cases} \dot{x}_1 = x_2 \\ \dot{x}_2 = a_1 x_4 x_6 + a_2 x_2^2 + a_3 \bar{\Omega}_r x_4 + b_1 (u_2 + f_{a1}) \\ \dot{x}_3 = x_4 \\ \dot{x}_4 = a_4 x_2 x_6 + a_5 x_4^2 + a_6 \bar{\Omega}_r x_2 + b_2 (u_3 + f_{a2}) \\ \dot{x}_5 = x_6 \\ \dot{x}_6 = a_7 x_2 x_4 + a_8 x_6^2 + b_3 (u_4 + f_{a3}) \\ \dot{x}_7 = x_8 \\ \dot{x}_8 = a_9 x_8 + \frac{1}{m} u_x u_1 \\ \dot{x}_9 = x_{10} \\ \dot{x}_{10} = a_{10} x_{10} + \frac{1}{m} u_y u_1 \\ \dot{x}_{11} = x_{12} \\ \dot{x}_{12} = a_{11} x_{12} - g + \frac{\cos(\phi)\cos(\theta)}{m} (u_1 + f_{a4}) \end{cases}$$

$$\begin{aligned} y = [&x_1 \quad x_2 + f_{s1} \quad x_3 \quad x_4 + f_{s2} \quad x_5 \quad x_6 + f_{s3} \\ &x_7 \quad x_8 + f_{s4} \quad x_9 \quad x_{10} + f_{s5} \quad x_{11} \quad x_{12} + f_{s6}]^T \end{aligned} \tag{11}$$

with

$$\begin{cases} a_1 = \left(\frac{I_y - I_z}{I_x}\right) \; a_2 = -\frac{K_{fax}}{I_x} \; a_3 = -\frac{J_r}{I_x} \; a_4 = \left(\frac{I_z - I_x}{I_y}\right) \; a_5 = -\frac{K_{fay}}{I_y} \\ a_6 = \frac{J_r}{I_y} \; a_7 = \left(\frac{I_x - I_y}{I_z}\right) \; a_8 = -\frac{K_{faz}}{I_z} \; a_9 = -\frac{K_{ftx}}{m} \; a_{10} = -\frac{K_{fty}}{m} \\ a_{11} = -\frac{K_{ftz}}{m} \; b_1 = \frac{l}{I_x} \; b_2 = \frac{l}{I_y} \; b_3 = \frac{1}{I_z} \end{cases} \tag{12}$$

The following assumptions are needed for the analysis,

Assumption 1: The velocity sensor faults are slowly varying in time, as follows:

$$\dot{f}_{si}(t) \approx 0, \quad \mathrm{i} \in [1,2,3,4,5,6] \tag{13}$$

Assumption 2: The resultant of actuator faults related to quadrotor motions and velocity sensor faults are bounded,

$$|f_{ai}(t)| \leq f_{ai}^{+} \text{ and } |f_{sj}(t)| \leq f_{sj}^{+} \quad , \quad \mathrm{i} \in [1,2,3,4] \text{ and } \mathrm{j} \in [1,2,3,4,5,6] \tag{14}$$

where $\{f_{a1}^{+}, f_{a2}^{+}, f_{a3}^{+}, f_{a4}^{+}\}$ and $\{f_{s1}^{+}, f_{s2}^{+}, f_{s3}^{+}, f_{s4}^{+}, f_{s5}^{+}, f_{s6}^{+}\}$ are positive constants.

Assumption 3: The unknowns parts $\gamma_{ai}(x, f_{ai}, t)$ including the resultants of actuator faults related to quadrotor motions, and $\gamma_{si}(x, f_{si}, t)$ related to velocity sensor faults are also bounded,

$$|\gamma_{ai}(x, f_{ai}, t)| \leq |g_i(x,t)| f_{ai}^{+} < k_{ai} \text{ and } |\gamma_{sj}(x, f_{sj}, t)| < k_{sj}, \mathrm{i} \in [1,2,3,4] \text{ and } \mathrm{j} \in [1,2,3,4,5,6] \tag{15}$$

where $\{k_{a1}, k_{a2}, k_{a3}, k_{a4}\}$ and $\{k_{s1}, k_{s2}, k_{s3}, k_{s4}, k_{s5}, k_{s6}\}$are also positive constants.

The adopted control strategy is based on two loops (internal loop and external loop). The internal loop contains four control laws: control of roll, control of pitch, control of yaw and control of altitude. The external loop includes two control laws of positions x and y. The external control loop generates a desired of roll (ϕ_d) and pitch (θ_d) through the correction block (illustrated by equation (4)). This block corrects the rotation of the roll and pitch depending on the desired yaw (ψ_d). The synoptic scheme below shows this control strategy:

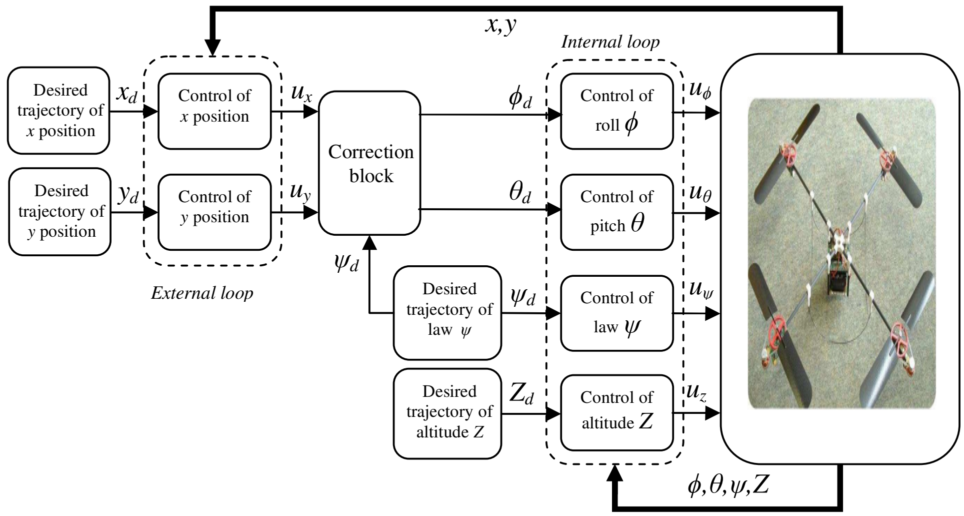

Figure 2. Synoptic scheme of the proposed control strategy

Basing on backstepping approach, a recursive algorithm is used to synthesize the control laws forcing the system to follow the desired trajectory in presence of actuator and velocity sensor faults, we simplify all stages of calculation concerning the tracking errors and Lyapunov functions in the following way:

$$e_i = \begin{cases} x_i - x_{id} & \text{i} \in [1,3,5,7,9,11] \\ y_i - \dot{x}_{(i-1)d} + c_{(i-1)} e_{(i-1)} - \varsigma_{(i-1)} & \text{i} \in [2,4,6,8,10,12] \end{cases} \tag{16}$$

and

$$\varsigma_i = \begin{cases} k_i \int_0^t e_i \, d\tau & \text{i} \in [1,3,5,7,9,11] \\ k_i \, sign(e_i) & \text{i} \in [2,4,6,8,10,12] \end{cases} \tag{17}$$

The corresponding lyapunov functions are given by:

$$V_i = \begin{cases} \frac{1}{2} e_i^2 + \frac{1}{2} e_{fj}^2 & \text{i} \in [1,3,5,7,9,11] \text{ and j} \in [1,...,6] \\ V_{i-1} + \frac{1}{2} e_i^2 & \text{i} \in [2,4,6,8,10,12] \end{cases} \tag{18}$$

such as

$$\begin{cases} e_{fj} = f_{sj} - \varsigma_i & \text{i} \in [1,3,5,7,9,11] \text{ and j} \in [1,...,6] \\ \Upsilon_j = \begin{pmatrix} c_i & k_i \\ 1 & 0 \end{pmatrix} > 0 & \text{i} \in [1,3,5,7,9,11] \text{ and j} \in [1,...,6] \\ c_i > 0 & \text{i} \in [2,4,6,8,10,12] \\ k_i > \left. \begin{cases} k_{sj} + k_{aj'} & \text{j} \in [1,2,3,6] \text{ and j'} \in [1,...,4] \\ k_{sj} & \text{j} \in [4,5] \end{cases} \right\} & \text{i} \in [2,4,6,8,10,12] \end{cases} \tag{19}$$

The synthesized stabilizing control laws are as follows:

$$\begin{cases} u_2 = \dfrac{1}{b_1}\left(\ddot{x}_{1d} - c_1(-c_1 e_1 + k_1\int_0^t e_1 d\tau + e_2) + (k_1 - 1)e_1 - c_2 e_2 - a_1 y_4 y_6 - a_2 y_2^2 - a_3\bar{\Omega}_r y_4 - k_2 sign(e_2)\right) \\ u_3 = \dfrac{1}{b_2}\left(\ddot{\theta}_d - c_3(-c_3 e_3 + k_3\int_0^t e_3 d\tau + e_4) + (k_3 - 1)e_3 - c_4 e_4 - a_4 y_2 y_6 - a_5 y_4^2 - a_6\bar{\Omega}_r y_2 - k_4 sign(e_4)\right) \\ u_4 = \dfrac{1}{b_3}\left(\ddot{\psi}_d - c_5(-c_5 e_5 + k_5\int_0^t e_5 d\tau + e_6) + (k_5 - 1)e_5 - c_6 e_6 - a_7 y_2 y_4 - a_8 y_6^2 - k_6 sign(e_6)\right) \\ u_x = \dfrac{m}{u_1}\left(\ddot{x}_d - c_7(-c_7 e_7 + k_7\int_0^t e_7 d\tau + e_8) + (k_7 - 1)e_7 - c_8 e_8 - a_9 y_8 - k_8 sign(e_8)\right) \quad /u_1 \neq 0 \\ u_y = \dfrac{m}{u_1}\left(\ddot{y}_d - c_9(-c_9 e_9 + k_9\int_0^t e_9 d\tau + e_{10}) + (k_9 - 1)e_9 - c_{10} e_{10} - a_{10} y_{10} - k_{10} sign(e_{10})\right) \quad /u_1 \neq 0 \\ u_1 = \dfrac{m}{\cos(x_1)\cos(x_3)}\left(\ddot{z}_d - c_{11}(-c_{11} e_{11} + k_{11}\int_0^t e_{11} d\tau + e_{12}) + (k_{11} - 1)e_{11} - c_{12} e_{12} - a_{11} y_{12} + g - k_{12} sign(e_{12})\right) \end{cases} \tag{20}$$

• ***Proof***

For *i* =1:

$$\begin{cases} e_1 = x_1 - x_{1d} \\ V_1 = \dfrac{1}{2}e_1^2 + \dfrac{1}{2}e_{f1}^2 \Big/ e_{f1} = f_{s1} - \varsigma_1 \end{cases} \tag{21}$$

and

$$\dot{V}_1 = e_1\dot{e}_1 + e_{f1}\dot{e}_{f1} = e_1\left((y_2 - f_{s1}) - \dot{x}_{1d}\right) + e_{f1}\left(-\dot{\varsigma}_1\right) \tag{22}$$

The stabilization of e_1 can be obtained by introducing a new virtual control y_2

$$\left(y_2\right)_d = \alpha_1 = \dot{x}_{1d} - c_1 e_1 + \varsigma_1 \big/ c_1 > 0 \tag{23}$$

Consequently,

$$\dot{V}_1 = e_1\left(-c_1 e_1 - e_{f1}\right) + e_{f1}\left(-\dot{\varsigma}_1\right) \tag{24}$$

In order to compensate the effect of the velocity sensor fault of roll motion, an integral term is introduced which can eliminate the tracking error. We take:

$$\varsigma_1 = k_{s1}\int_0^t e_1 d\tau \tag{25}$$

It results that:

$$\dot{V}_1 = e_1\left(-c_1 e_1 - e_{f1}\right) + e_{f1}\left(-k_1 e_1\right) = -\left(e_1 \quad e_{f1}\right)\begin{pmatrix} c_1 & 1 \\ k_1 & 0 \end{pmatrix}\begin{pmatrix} e_1 \\ e_{f1} \end{pmatrix} = -\bar{e}_1^T \Upsilon_1 \bar{e}_1 \tag{26}$$

c_1 and k_1 are chosen so as to make the matrix Υ_1 positive definite, which means that, $\dot{V}_1 \leq 0$

For *i* =2:

$$\begin{cases} e_2 = y_2 - \dot{x}_{1d} + c_1 e_1 - \varsigma_1 \\ V_2 = V_1 + \frac{1}{2} e_2^2 \end{cases} \tag{27}$$

and

$$\begin{aligned} \dot{V}_2 &= e_1\left(-c_1 e_1 - e_{f1} + e_2\right) + e_{f1}\left(-k_1 e_1\right) \\ &+ e_2\left(a_1 y_4 y_6 + a_2 y_2^2 + a_3 \bar{\Omega}_r y_4 - \ddot{x}_{1d} + c_1(-c_1 e_1 + \varsigma_1 + e_2) - k_1 e_1 + \gamma_{a1} + \gamma_{s1} + b_1 u_2\right) \end{aligned} \tag{28}$$

We know a priori from (15) and (19.d) that:

$$|\gamma_{s1}| + |\gamma_{s1}| = b_1 |f_{a1}| + \left|-c_1 f_{s1} - a_1(f_{s3} y_4 + f_{s2} y_6 - f_{s2} f_{s3}) - a_2(f_{s1} y_2 - f_{s1}^2) - a_3 \bar{\Omega}_r f_{s2}\right| < k_2 \tag{29}$$

The stabilization of (e_1, e_2) can be obtained by introducing the input control u_2

$$u_2 = \frac{1}{b_1}\left(\ddot{x}_{1d} - c_1(-c_1 e_1 + \varsigma_1 + e_2) + (k_1 - 1)e_1 - c_2 e_2 - a_1 y_4 y_6 - a_2 y_2^2 - a_3 \bar{\Omega}_r y_4 - \varsigma_2\right) \Big/ c_2 > 0 \tag{30}$$

It result that

$$\dot{V}_2 = -\bar{e}_1^T \Upsilon_1 \bar{e}_1 - c_2 e_2^2 - e_2\left(\varsigma_1 - \left(\gamma_{a1} + \gamma_{s1}\right)\right) \tag{31}$$

In order to compensate the unknown parts ($\gamma_{a1} + \gamma_{s1}$), a “sign” function is introduced. We take:

$$\varsigma_2 = k_2 sign(e_2) \tag{32}$$

By using the compensation term (32) and the equation (31) it comes

$$\dot{V}_2 \le -\bar{e}_1^T \Upsilon_1 \bar{e}_1 - c_2 e_2^2 - |e_2|(k_2 - |\gamma_{a1} + \gamma_{s1}|) \le 0 \tag{33}$$

The same steps are followed to extract u_3, u_4, u_x, u_y and u_1.

It is well known that sliding mode control signal is discontinuous in nature on the switching manifold, which in duces a chattering phenomenon. To avoid the effect of this phenomenon, the sign function can be replaced by another function called “saturation function sat(.)”, it’s is given by:

$$sat(e) = \begin{cases} \frac{e}{\Phi} & \text{if } |e| \le \Phi \\ sign(e) & \text{else} \end{cases} \tag{34}$$

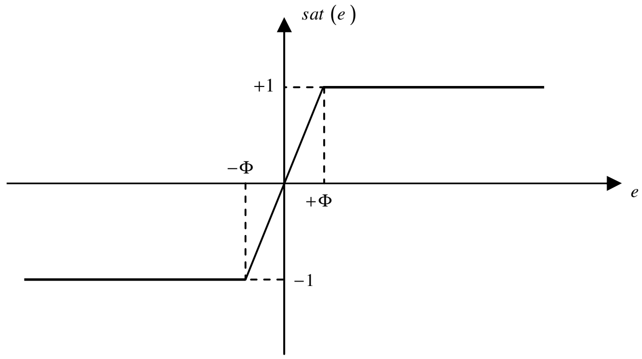

Figure. 3. Saturation function “sat(.)”.

4. SIMULATION RESULTS

In order to see the performances of the controller developed in this paper, two tests are treated.

1- Results without faults are shown in Figure. 4, Figure. 6, Figure. 8 and Figure .10.a.

2- Results with four sensor faults $\{f_{s1}, f_{s2}, f_{s3}, f_{s6}\}$ added in angular velocities and linear velocity of altitude with 50% of these maximum values and four resultants of actuator faults $\{f_{a1}, f_{a2}, f_{a3}, f_{a4}\}$ related to roll, pitch, yaw and altitude motions with 20% of these maximum values at 5s, 9s, 12s, 15s, 20s, 24s, 27s and 30s respectively are shown in Figure. 5, Figure. 7, Figure. 9 and Figure.10.b.

The simulation results are obtained based on the following real parameters in Table. 1:

Table 1. Quadrotor parameters.

Parameter	Value
m	0.486 kg
g	9.806 m/s^2
l	0.25 m
b	2.9842×10^{-5} $N/rad/s$
d	3.2320×10^{-7} $N.m/rad/s$
J_r	2.8385×10^{-5} $kg.m^2$
$I_{(x,y,z)}$	$diag$ (3.8278, 3.8278, 7.1345) $\times 10^{-3}$ $kg.m^2$
$K_{fa(x,y,z)}$	$diag$ (5.5670, 5.5670, 6.3540) $\times 10^{-4}$ $N/rad/s$
$K_{ft(x,y,z)}$	$diag$ (0.0320, 0.0320, 0.0480) $N/m/s$
k_m	4.3×10^{-3} $N.m/A$
k_g	5.6
R_a	0.67 Ω

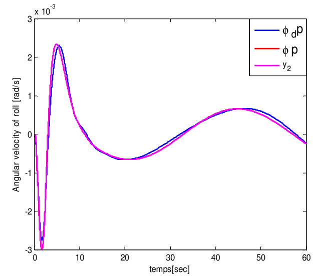

(a) evolution of angular velocity of roll

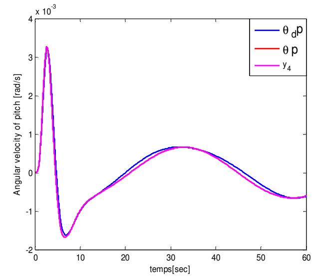

(b) evolution of angular velocity of pitch

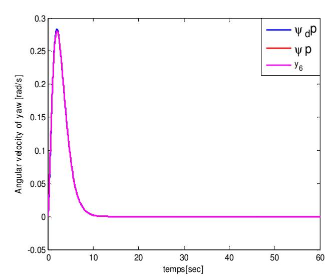

(c) evolution of angular velocity of yaw

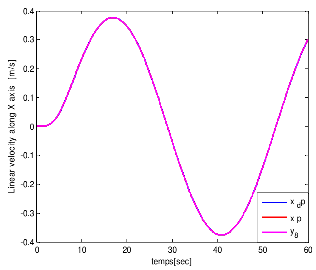

(d) evolution of linear velocity along *X* axis

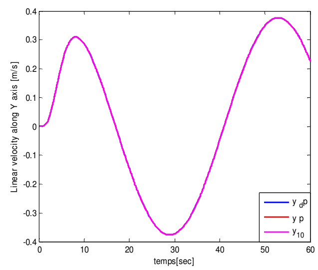

(e) evolution of linear velocity along *Y* axis

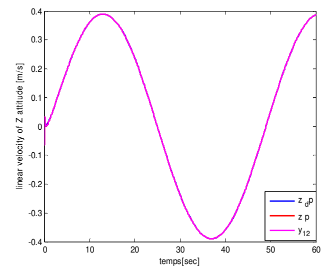

(f) evolution of linear velocity along *Z* axis

Figure. 4. Tracking simulation results of angular and linear velocities, Test 1.

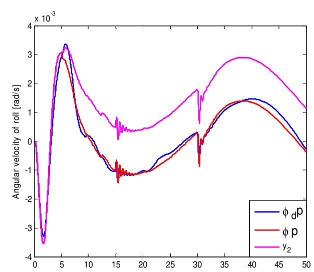

(a) evolution of angular velocity of roll

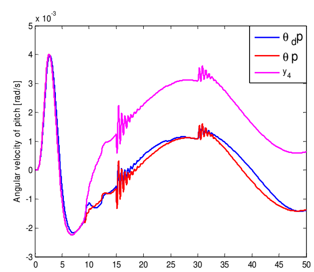

(b) evolution of angular velocity of pitch

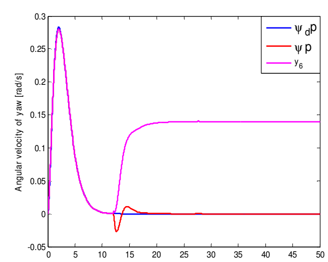

(c) evolution of angular velocity of yaw

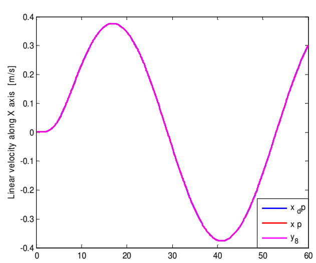

(d) evolution of linear velocity along *X* axis

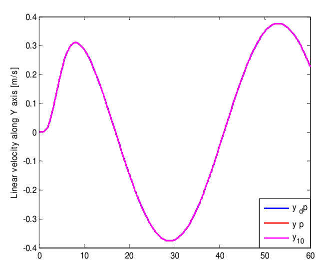

(e) evolution of linear velocity along *Y* axis

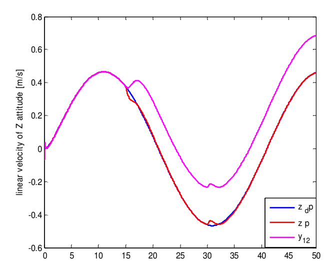

(f) evolution of linear velocity along *Z* axis

Figure. 5. Tracking simulation results of angular and linear velocities, Test 2.

Figure. 4 and Figure. 5 represents the quadrotor velocities, It can be seen a good tracking of the desired velocities in Figure. 4, with tracking deviation in the measurements of angular velocities and linear velocity of altitude with 50% of her maximum values in Figure. 5 (illustrated respectively by (a), (b), (c), and (f)) due after occurrence of these corresponding sensor faults, we can see also from this figure a transient peaks in roll, pitch and altitude velocities caused by the appearance of velocity sensor fault of altitude at 15s and resultants of actuator faults related to altitude motion at 30s, which gives us a wrong information of velocities of our system.

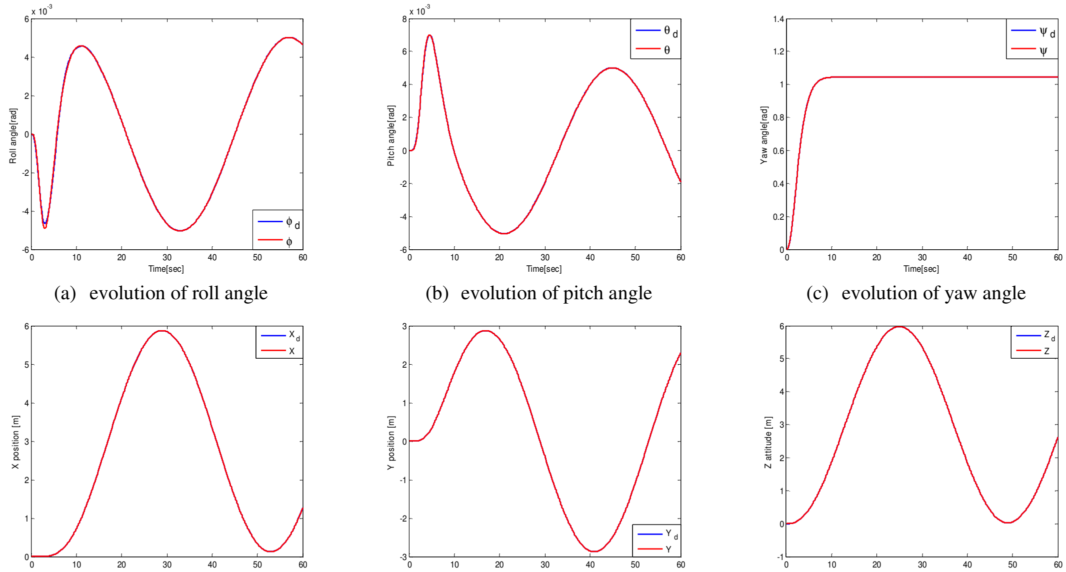

(a) evolution of roll angle (b) evolution of pitch angle (c) evolution of yaw angle

(d) evolution of x position (e) evolution of y position (f) evolution of z position

Figure. 6. Tracking simulation results of trajectories along roll (ϕ), pitch (θ), yaw angle (ψ) and (X,Y,Z) axis, Test 1.

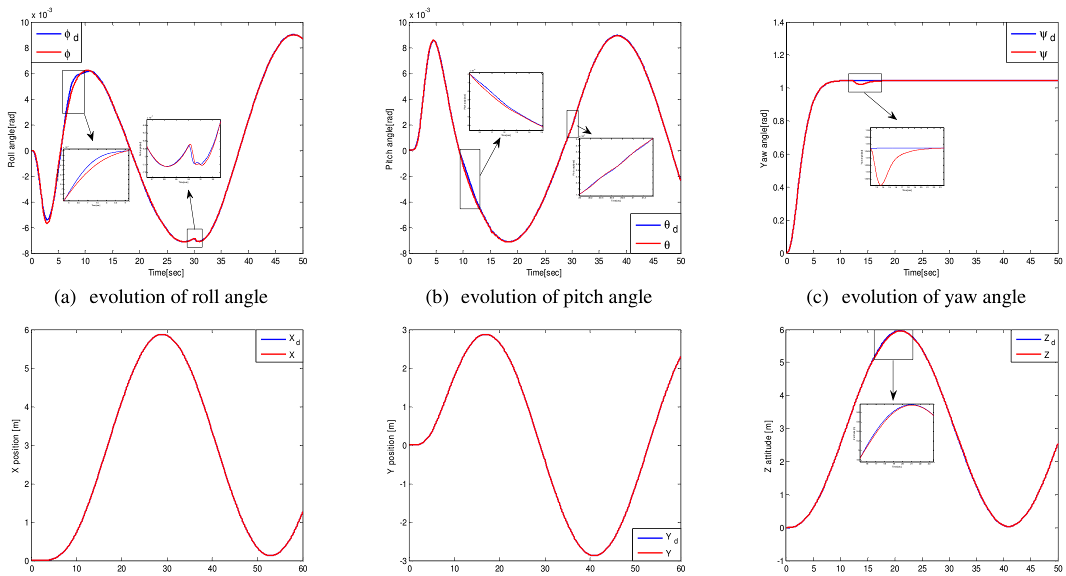

(a) evolution of roll angle (b) evolution of pitch angle (c) evolution of yaw angle

(d) evolution of x position (e) evolution of y position (f) evolution of z position

Figure. 7. Tracking simulation results of trajectories along roll (ϕ), pitch (θ), yaw angle (ψ) and (X,Y,Z) axis, Test 2.

Figure. 6 and Figure. 7 represents the quadrotor trajectories. From these figures, we can see well a good tracking of the desired trajectories, with small transient deviations in roll, pitch, yaw and altitude motions given by Figure. 7 (illustrated respectively by (a), (b), (c), and (f)) caused by appearance of the corresponding velocity sensor faults, we can see also from this figure another deviations in roll and pitch motions due after occurrence of the resultant of actuator faults related to altitude motion. Despite that, the trajectories tracking of our system is assured.

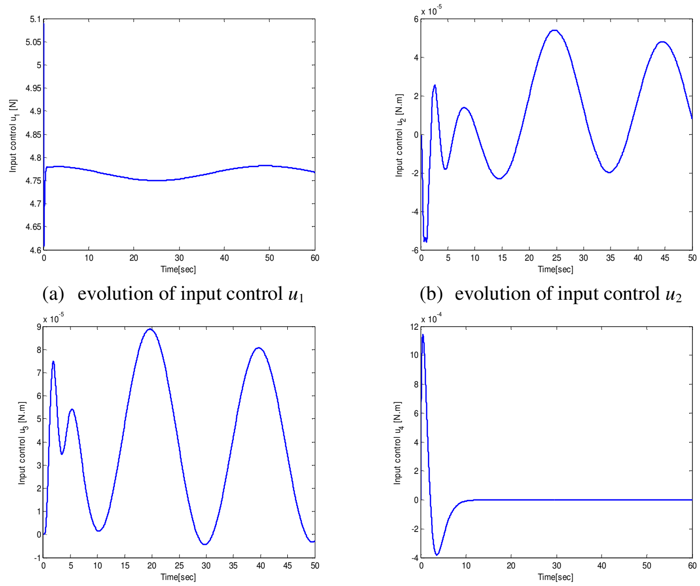

(a) evolution of input control u_1 (b) evolution of input control u_2

(c) evolution of input control u_3 (d) evolution of input control u_4

Figure. 8. Simulation results of all controllers, Test 1.

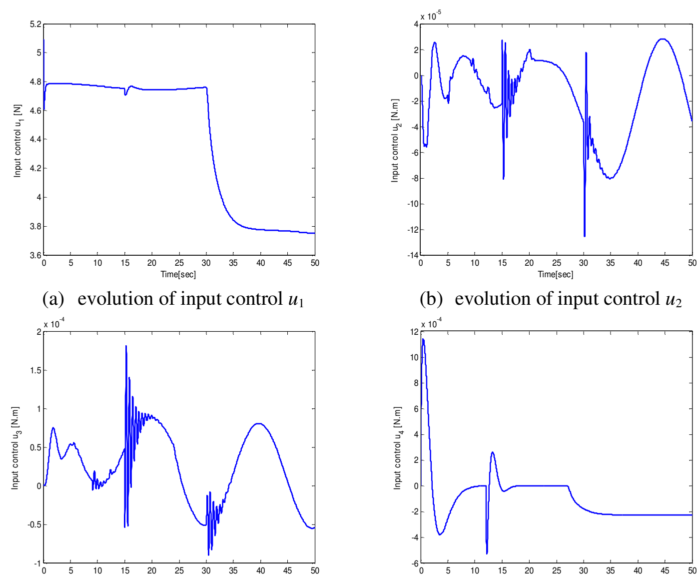

(a) evolution of input control u_1 (b) evolution of input control u_2

(c) evolution of input control u_3 (d) evolution of input control u_4

Figure. 9. Simulation results of all controllers, Test 2.

Figure. 8 and Figure. 9 represents the inputs control $\{u_1, u_2, u_3, u_4\}$ of our system. From Figure. 9, it is clear to see the transient peaks in all controllers, especially in inputs control u_2 and u_3 (illustrated by (b) and (c)). Furthermore, we can see well a considerable deviation in evolution of inputs control u_4 and u_1 (illustrated by (d) and (a)) after 27s and 30s caused by occurrence of the resultant of actuator faults related respectively to yaw and altitude motions. Despite that, the stability of the closed loop dynamics of quadrotor is guaranteed. We can see also that the obtained input control signals given by this control strategy are acceptable and physically realizable.

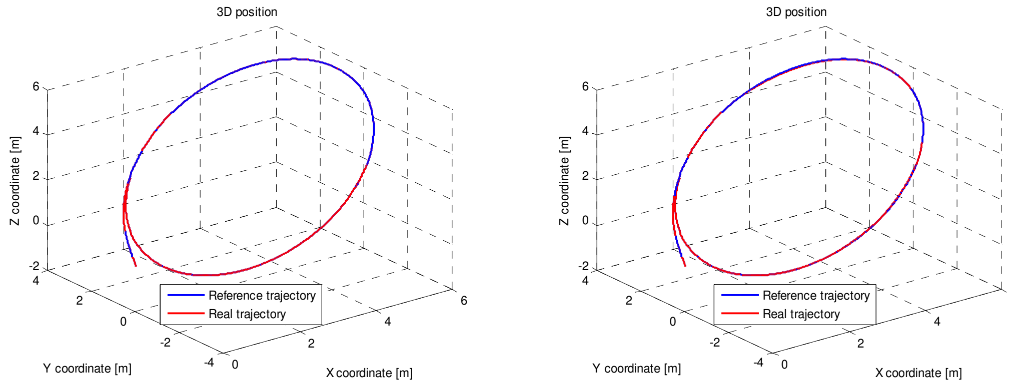

(a) evolution of position along (*X*,*Y*,*Z*) axis, Test 1 (b) evolution of position along (*X*,*Y*,*Z*) axis, Test 2

Figure. 10. Global trajectory of quadrotor in 3D.

Figure. 10 represents the 3D position of quadrotor aircraft during the flight. The simulation results given by this figure shows a good performances and robustness towards stability and tracking even after occurrence of actuator and velocity sensor faults, which explains the efficiency of control strategy developed in this paper.

5. CONCLUSIONS AND FUTUR WORKS

In this paper, we proposed a new control strategy based on robust integral backstepping using sliding mode and taking into account the actuator and sensor faults. Firstly, we presented the dynamical model of the quadrotor taking into account the different physics phenomena which can influence the evolution of our system in the space. Secondly, we synthesized a stabilizing control laws in presence of simultaneous actuator and sensor faults. The simulation results have shown high efficiency of this control strategy, its main advantage is to keep at same time the stability and the performances of quadrotor during a malfunction of these actuators and velocity sensors. As prospects we hope to implement this control strategy on a real system.

6. REFERENCES

[1] P. Adigbli, C. Grand, J. B. Mouret, & S. Doncieux. (2007) “Nonlinear attitude and position control of a micro quadrotor using sliding mode and backstepping techniques”, *Conference and Flight Competition (EMAV)*, France, pp. 1-9.

[2] S. Bouabdellah, & R.Siegwart. (2005) “Backstepping and sliding mode techniques applied to an indoor micro quadrotor”, *Proceeding of the IEEE, ICRA*, Barcelona, Spain, pp. 2259-2264.

[3] H. Bouadi, M. Bouchoucha, & M. Tadjine. (2007) “Modelling and Stabilizing Control Laws Design Based on Backstepping for an UAV Type-Quadrotor”, *Proceeding of 6th IFAC Symposium on IAV*, Toulouse, France.

[4] H. Bouadi, M. Bouchoucha, & M. Tadjine. (2007) “Sliding Mode Control Based on Backstepping Approach for an UAV Type-Quadrotor”, *International Journal of Applied Mathematics and Computer Sciences*, Vol. 4, No. 1, pp. 12-17.

[5] H .Bouadi, S. Simoes Cunha, A. Drouin, & F. Mora-Camino. (2011) “Adaptive Sliding Mode Control for Quadrotor Attitude Stabilization and Altitude Tracking” *Proceeding of 12th IEEE International Symposium on Computational Intelligence and Informatics*, Budapest, Hungary, pp. 449-455.

[6] M. Bouchoucha, M. Tadjine, A. Tayebi, & P. Müllhaupt. (2008) “Step by Step Robust Nonlinear PI for Attitude Stabilization of a Four-Rotor Mini-Aircraft”, *Proceeding of 16th Mediterranean Conference on Control and Automation Congress Centre*, Ajaccio, France, pp. 1276-1283.

[7] M. Bouchoucha, S. Seghour, & M. Tadjine. (2011) "Classical and Second Order Sliding Mode Control Solution to an Attitude Stabilization of a Four Rotors Helicopter: from Theory to Experiment", *Proceeding of the IEEE Conference on Mechatronics*, Istanboul, Turkey, pp. 162-169.
[8] P. Castillo, A. Dzul, & R. Lozano. (2004) "Real-Time Stabilization and Tracking of a Four-Rotor Mini Rotorcraft", *IEEE Transactions on Control Systems Technology*, Vol. 12, No. 4, pp. 510-516.
[9] J. Colorado, A. Barrientos, , A. Martinez, B. Lafaverges, & J. Valente. (2010) "Mini-quadrotor attitude control based on Hybrid Backstepping & Frenet-Serret Theory", *Proceeding of the IEEE, ICRA*, Anchorage, Alaska, USA, pp. 1617-1622.
[10] A. Das, F. Lewis, K. Subbarao (2009) "Backstepping Approach for Controlling a Quadrotor Using Lagrange Form Dynamics." *Journal of Intelligent and Robotic Systems*, Vol. 56, No. 1-2, pp. 127-151.
[11] L. Derafa, T. Madani, & A. Benallegue. (2006) "Dynamic modelling and experimental identification of four rotor helicopter parameters", *IEEE-ICIT* , Mumbai, India, pp. 1834-1839.
[12] N. Guenard, T. Hamel, & R. Mahony. (2008) "A Practical Visual Servo Control for an Unmanned Aerial Vehicle", *IEEE Transactions on Robotics*, Vol. 24, No. 2, pp. 331-340.
[13] M. Huang, B. Xian, C. Diao, K. Yang, & Y. Feng. (2010) "Adaptive tracking control of underactuated quadrotor unmanned aerial vehicles via backstepping", *Proceeding of American Control Conference*, Baltimore, USA, pp. 2076-2081.
[14] R. Lozano, P. Castillo, & A. Dzul. (2004) "Global stabilization of the PVTOL: real time application to a mini aircraft", *International Journal of Control*, Vol 77, No 8, pp. 735-740.
[15] T. Madani & A. Benallegue. (2006) "Backstepping control for a quadrotor helicopter", *Proceeding of the IEEE Conference on Intelligent Robots and Systems*, pp. 3255-3260.
[16] T. Madani & A. Benallegue. (2006) "Backstepping Sliding Mode Control Applied to a Miniature Quadrotor Flying Robot", *Proceeding of the IEEE Conference on Industrial Electronics*, pp. 700-705.
[17] C. Nicol, C. J. B. Macnab, & A. Ramirez-Serrano. (2008) "Robust neural network control of a quadrotor helicopter" *Proceeding of the IEEE Canadian Conference on Electrical and Computer Engineering*, pp. 1233-1237.
[18] S. Seghour, M. Bouchoucha, & H. Osmani. (2011) "From Integral Backstepping to Integral Sliding Mode Attitude Stabilization of a Quadrotor System: Real Time Implementation on an Embedded Control System Based on a dsPIC µC", *Proceeding of the IEEE Conference on Mechatronics*, Istanboul, Turkey, pp. 154-161.
[19] J.J.E. Slotine, & W. Li. (1991) "Applied nonlinear control", Prentice Hall, Englewood Cliffs, NJ.
[20] A. Tayebi, & S. McGilvray. (2006) "Attitude stabilization of a VTOL Quadrotor Aircaft", *IEEE Transactions on Control Systems Technology*, Vol. 14, No. 3, pp. 562-571.

Authors

Hicham KHEBBACHE is a Graduate student (Magister) of Automatic Control at the Electrical Engineering Department of Setif University, Algeria. He received the Engineer degree in Automatic Control from Jijel University, Algeria, in 2009. He is with Automatic Laboratory of Setif (LAS). His research interests include Aerial robotics, Linear and Nonlinear control, Robust control, F ault tolerant control (FTC), Diagnosis, Fault detection and isolation (FDI).

Belkacem SAIT is an Associate Professor at Setif University and member at Automatic Laboratory of Setif (LAS), Algeria. He received the Engineer degree in Electrical Engineering fro m National Polytechnic school of Algiers (ENP) in 1987, the Magister degree in Instrumentation and Control from HCR of Algiers in 1992, and the Ph.D. in Automatic Product from Setif University in 2007. His research interested include discrete event systems, hybrid systems, Petri nets, Fault tolerant control (FTC), Diagnosis, Fault detection and isolation (FDI).

Naâmane BOUNAR is a Ph.D. student at the Automatic Control Department of Jijel University and member at Automatic Laboratory of Jijel (LAJ), Algeria**.** He received the Engineer degree in Automatic Control from Jijel University, Algeria, in 2000, and the Magister degree in Robotics, Automatic and Industrial Informatics from Military Polytechnic School (EMP), Algiers, in 2004, since 2005, he has been an Assistant professor at the Department of Automatic Control, Jijel University, Algeria. His research interests include robotics, sliding mode control, intelligent control and application of modern control theory to electrical machines.

Fouad YACEF is currently a Ph.D. student at the Automatic Control Department of Jijel University, Algeria. He received the Engineer degree in Automatic Control from Jijel University, Algeria, in 2009, and the Magister degree in Control and Command from Military Polytechnic School (EMP), Algiers, in November 2011. He is with Automatic Laboratory of Jijel (LAJ). His research interests include Aerial robotics, Linear and Nonlinear control, LMI optimisation, Analysis and design of intelligent control systems.